Embedding Ionic Hydrogel in 3D Printed Human-Centric Devices for Mechanical Sensing

Baanu Payandehjoo

A Thesis

in the Department of

Mechanical, Industrial and Aerospace Engineering

Presented in Partial Fulfillment of the Requirements

for the Degree of Master of Sciences (Mechanical Engineering)

at Concordia University

Montreal, Quebec, Canada

August, 2023

Declaration of Authorship

This is to certify that the thesis prepared

By: Baanu Payandehjoo

Entitled: Embedding Ionic Hydrogel in 3D Printed Human-Centric Devices for Mechanical Sensing

and submitted in partial fulfillment of the requirements for the degree of

Master of Applied Science in Mechanical Engineering

complies with the regulations of the University and meets the accepted standards with respect to originality and quality.
Signed by the Final Examining Committee:

Dr. Muthukumaran Packirisamy Chair

Dr. Muthukumaran Packirisamy Examiner

Dr. Lyes Kadem Examiner

Dr. Tsz Ho Kwok Supervisor

Approved by: _____

Sivakumar Narayanswamy, Graduate Program Director

Date: _____

Mourad Debbabi, Dean of Faculty

Abstract

Gina Cody School of Engineering and Computer Science

Mechanical, Industrial and Aerospace Engineering

Master of Applied Science

Embedding Ionic Hydrogel in 3D Printed Human-Centric Devices for Mechanical Sensing

by Baanu Payandehjoo

Flexible sensor applications have increasingly focused on ionically conductive hydrogels due to their notable deformability and easily tunable properties compared to rigid materials. These hydrogels possess electrical properties, thanks to their high water content and porous structure that facilitate effective ion transfer. Despite their attractive features, hydrogels have limitations in terms of water retention and shape fidelity, and they are more typically inspected as two dimensional films and patches. In this paper, 3D printed thermoplastic polyurethane (TPU) elastomer frames with various geometries were injected with ionic conductive polyacrylamide (PAAm) based hydrogels to create durable, robust soft mechanical sensors for detecting strain, pressure, and bending through changes in their electrical resistance. After the effectiveness of the TPU encasement in maintaining the hydrogel water content was demonstrated, hydrogel embedded frames with varying geometries were designed. Their response to mechanical loading was investigated in relation to their dimensions and geometric shape. Finally, glove-shaped frames were fabricated to fit human fingers and injected with ionic hydrogel for sensing abilities. The wearable sensors accommodated free movement of the fingers in multiple directions and were able to detect simultaneous and independent bending and stretching of the fingers. Through comprehensive observation of the electrical behavior of all soft ionic sensors in response to different kinds of mechanical stimuli, it was concluded that the resistance change following mechanical loading was dependent on the specific geometric features of each individual hybrid sensor. Thus, ionic hydrogel-embedded TPU encasement could be designed with targeted geometry to dictate the type and direction of mechanical sensing with

regard to its application. This work presents a facile approach to fabricating multi-component soft geometric sensors with potential to be used for wearable electronics and human-machine interactions.

Acknowledgements

I would like to acknowledge everyone who helped me during my degree. Christopher-Denny Matte for taking the time and effort to share with me his experience in the lab. My parents and friends for their unwavering support and encouragement. Finally, I would like to thank my supervisor, Tsz Ho Kwok, for his invaluable guidance throughout the process of my Master's degree, and for consistently encouraging me to exercise independent and creative thinking in my research.

Contents

List of Figures

List of Tables

Chapter 1

Introduction

Flexible electronics have been gaining increasing attention among researchers following the advancement of human-machine interactions in a myriad of areas, such as soft robotics, wearable electronics, and personal healthcare monitoring [1–3]. Although rigid materials are more deeply understood and have better electrical performance, flexible components can better accommodate large, repeated deformations and conform to non-conventional surfaces. The expanding pool of information on flexible stimuli-responsive devices has shown their potential in fields where stretchability, transparency, and biocompatibility are key, while rigid electronics struggle to comply [4]. When it comes to such human-centric applications, not only is high ranges of deformability come into play, but safety in use also becomes an important concern.

Hydrogels have shown great promise in fulfilling these criteria, especially because of their mechanical properties that closely resemble biological tissue [5]. Known as one of the most workable examples of soft materials, hydrogels are three-dimensional (3D) polymer networks that contain water within their structure. Over the past few decades, they have been extensively used in the biomedical field both as invasive and non-invasive devices, and their usage persists to this day [6, 7], contact lenses being one of the most prominent examples.

Due to their aqueous nature, hydrogels are soluble in water and must be reinforced with additional physical and chemical crosslinks, including hydrogen bonds and ionic complexation. Their hydrophilic behavior enables the absorption of water and ionic solutions by the free volume between the polymer chains, which endow conductivity through ion migration akin to biological tissue. Because of their significant water content and porous structure, ionic hydrogels can undergo large deformations under

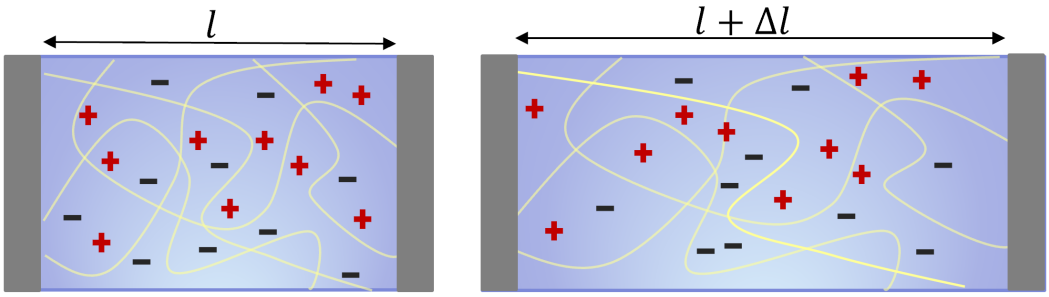

FIGURE 1.1: Ionic hydrogel chain rearrangement under loading

mechanical stimuli, such as strain, pressure, bending, and even smaller forces, like vibration. Changes in the material dimensions alter pathways through which the ions move (Fig. 1.1), correspondingly changing its conductance and supplying it with sensing abilities [8–10]. This electrical behavior can be tracked by placing the conductive hydrogels in a circuit, in which an electronic double layer (EDL) couples the ionic current in the hydrogel and the electronic current in the metal wires [11].

Regarding the performance of hydrogel ionotronics, the steps to fabricate the devices are as central as the electronics portion of the process. Changing the main and auxiliary constituents of the polymer solution and polymerization parameters can help control some characteristics of the final hydrogel product, which grants them a significant advantage in the tunability of their performance [12].

One of the most persistent issues typically encountered when dealing with hydrogels is their low water retention. Without sufficient binding of the water molecules to the polymeric structure of the porous hydrogels, water evaporates from their surface, essentially altering the material properties. The rate of water loss —as well as many other hydrogel properties— depends on multiple factors including but not limited to the types of monomers used, supplementary crosslinks and sacrificial bonds, polymerization technique, and environmental conditions during fabrication [13–16]. For example, some research add hydratable salts to the hydrogel to help keep the water content. However, this approach can only slow down the evaporation a bit, the hydrogel still eventually dries up [17]. Similar methods could be implemented to modify the mechanical properties of the hydrogels, such as their stiffness (Young's Modulus) which creates obstacles for their 3D fabrication [18].

Although hydrogels have many attractive features and have shown potential towards being 3D printed [19–21], they are still usually inspected as two-dimensional components like skin-like films and patches due to their limited structural stiffness [22] and are mostly used underwater or in vivo where they can retain water content more efficiently. While their aqueous nature results in favorable ductility and permeability, they simultaneously bound their ability to hold stable, irregular shapes, especially on larger scales [18]. In addition, the high surface-area-to-volume ratio of a complex shape increases the rate of water evaporation from the hydrogels when they expose to the ambient environment. The water content is the primary means of ion transport inside the porous structure and correlates directly with its conductive properties.

Finding a proper balance in hydrogels can be a laborious task. Their deformability, strength, conductivity, and water retention are all highly interdependent, and changing one factor in the fabrication process can compromise others entirely. For example, the mechanical support of a hydrogel for fabrication in three-dimensional geometries can be enhanced by increasing the bonds and entanglements between its chains, resulting in a stiffer structure. However, this tighter packing of the hydrogel also leads to smaller pore sizes, restricting the medium for ion transport. As a consequence, the bulk conductivity of the ionic hydrogel is reduced [23]. With the growing interest in flexible electronics and personalized functional products, there is a need to make hydrogels long-lasting and more structurally robust in ambient working conditions.

The traditional way of fabricating hydrogels is molding, where the hydrogel is injected into and solidified in a mold [24, 25]. The mold is unwanted and will be peeled off to release the hydrogel. However, it can be observed that electronics are seldom alone. They are usually made up of components with specific functionalities collectively acting toward a common goal. For example, a printed circuit board — already consisting of multiple components mounted onto a substrate— is encased in a shell to make a functional mouse. Instead of creating a separate mold to shape the hydrogel, an alternative approach was proposed to design the mold as an integral part of the device. This design allows the mold and the hydrogel to function together, aiming to develop a hydrogel sensor capable of incorporating geometrical complexities during fabrication. The resulting sensor is expected to possess long-lasting properties, enhancing practicality for real-life applications.

Specifically, a hybrid hydrogel-elastomer strain sensor is developed. Through 3D printing, custom hollow frames are fabricated with various geometries using thermoplastic polyurethane (TPU). Photopolymerizable ionic hydrogel solution is then injected into the frame structures and UV-cured to get the final conductive elastomer. Afterward, the soft conductors are used as sensors, which transduce mechanical stimuli into electrical signals to identify strain, pressure, and bending. In this way, the mold could protect the hydrogel from water loss and also provide support for the hydrogel to have a higher shape complexity.

The objective of this thesis is to test this proposed method and answer the following questions:

- What process should be used to encase the hydrogel?
- How effective will the encasement be in terms of increasing water retention and shape fidelity?
- How will the encasement affect the mechanosensitivity of the hydrogel?
- What design parameters and geometries will accommodate sensing of specific mechanical stimuli?

The experimental results show the potential of these hydrogel-embedded complex elastomer geometries to be used in wearable electronics and human-machine interactions.

The rest of the paper is organized as follows. In Chapter 2, related works will be presented. Chapter 3 will outline the preparation and characterization steps of the materials along with the methodology leading to custom- designed stretchable conductor. The evaluation of the samples in terms of water retention, complex geometry, and electrical behavior will be discussed in Chapters 4 and 5. Finally, Chapter 6 includes the analysis and discussion of experimental results, followed by a conclusion in Chapter 7.

Chapter 2

Literature Review

2.1 Ionic Hydrogels

Although hydrogels themselves show some electrical properties due to the presence of ions in fresh water, the addition of fillers significantly enhances their electrical response to mechanical stimuli. Some research have presented electrically conductive hydrogels using different approaches, such as constructing hydrogel nanocomposites by the addition of reinforcing fillers (e.g. CNTs and MXenes) or combining the hydrogel backbone with conductive polymers as interpenetrating polymer networks to develop flexible mechanical sensors in the biomedical sector [26–29].

Among many of these approaches, apprehensions arise regarding the safety implications associated with the everyday use of these conductive hydrogels. when it comes to human-centric applications where sensors are meant to come into direct contact with biological tissue, transparency, safety and biocompatibility are properties of the material that should be taken into careful consideration. In 2014, Sun et al. [30] presented a type of artificial skin in the form of ion-charged hydrogel structures called Ionic Skin (or I-Skin) by adding sodium chloride (NaCl) to their composition. Ever since, many have reported using different types of salts to provide hydrogels with electrical conductivity. Ionic hydrogels have shown to be more suitable for everyday use by humans. They exhibit electrical properties akin to biological tissue, in which sensory signals are also carried by ionic charge.

According to the Born theory and Born equation (Eq. 2.1), with the addition of ions to a solution, an electrostatic component of Gibbs free energy of solvation of an ion is added to the total energy of the system, fundamentally altering its thermodynamic

properties [31, 32].

$$\Delta G = -\frac{N_A z^2 e^2}{8\pi\epsilon_0 r_0} \tag{2.1}$$

Consequently, the inclusion of salts in the hydrogel composition can enhance their water retention abilities among others, directly influencing their mechanical and electrical behavior [33].

2.2 Applications of Hydrogel Mechanical Sensors

Leveraging the multifaceted properties of salts as suppliers of ionic conduction, many works present hydrogel strain sensors by adding KCl, LiCl, sodium casein, $Na_2B_4O_7$ and other salts to their composition, either as free ions [34–36] or crosslinked ions [37, 38]. With the same approach, Zhao et al. demonstrate a mechanically responsive ionic hydrogel sensor exhibiting resistance change following bending, stretching and pressing (shown in Figs. 2.1a-c). As shown in Figs. 2.1d-g, the hydrogel was able to act as a switch to turn on and off an LED while mounted on a hand [39]. Similarly, Jiang et al. use ionic crosslinking of $FeCl_3$ salt to the polymer backbone to enhance the recoverability and mechanical properties of the conductive hydrogel. The final sample is shown to respond in real-time to human motion, demonstrating capabilities to be applied in artificial intelligence and vocal rehabilitation training [40]. Many other ionic hydrogels investigated for biologically matched electronic interfaces show potential to be used for energy storage devices [41, 42], medical diagnostics and sports assistance [43, 44], and flexible touchscreen and handwriting interactions [45, 46].

With the vast potential of conductive hydrogels for application in a diverse range of technological domains arises the need to extend their reliability and longevity. The following sections of this chapter will cover the methods investigated to enhance the water retention ability and subsequently the durability of ionic hydrogels, as well as their shape fidelity and 3D fabrication.

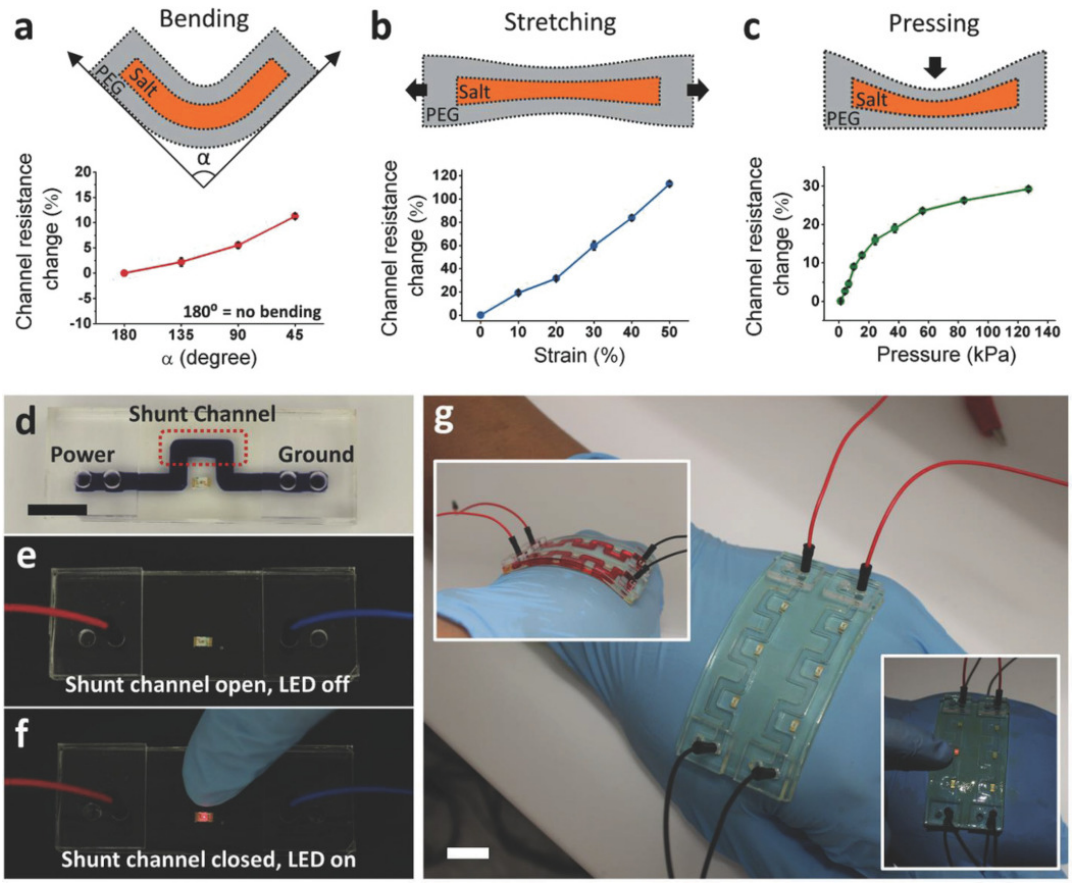

FIGURE 2.1: Mechanically responsive and reprogrammable hydrogel ionic circuits [39].

2.3 Water Retention and Life Cycle

Besides providing hydrogels with ionic conductivity, hygroscopic salts have been shown to reduce vapor pressure and slow down moisture evaporation by creating additional crosslinks and reducing pore size within the polymer structure. These extra crosslinks can also act as dynamic sacrificial bonds, contributing to the strength and toughness of the hydrogel [47]. Although it is a simple and effective way to enhance their durability, their behavior remains highly dependent upon environmental conditions, and most of them still face barriers in practical long-term applications [17, 48]. Sui et al. [48] used LiCl to fabricate an ionic conductive hydrogel with the ability to retain its water content after a week in ambient conditions. Multivalent salts such as $FeCl_3$ have been used for higher conductivity due to the higher number of free ions they release, as well as restricting water evaporation. This is because the Fe^{+} and Cl^{-} ions create additional crosslinks in the hydrogel structure, leading to smaller pores where charge

passes through [49].

Other than salts, the incorporation of various biopolymers including chitosan [50], agar [51], and cellulose nano-crystals [52] into the hydrogel composition has also been explored to enhance the strength and toughness of the gels. By introducing these biopolymers, non-covalent bond interactions are formed which enhance the strength and toughness of the structure, as described by Ahmadi et al. [53]. The inclusion of this biopolymer in the hydrogel solution leads to an increase in crosslink density of the polymer network, resulting in a higher viscosity of the solution.

Another approach to minimizing water loss from hydrogel surfaces is covering them with a protective layer, most commonly VHB tape [54]. Adding a hydrophobic polymer coating to the hydrogels creates a barrier against water evaporation and helps keep hydrogel properties steady and long-lasting. On the other hand, this method still limits the hydrogel shapes to relatively simple geometries and also complicates fabrication by creating additional assembly steps. Hydrophobic silicone-based coatings like polydimethylsiloxane (PDMS) and (3-aminopropyl) triethoxysilane (APTES) are examples of polymers used to shield the hydrogel surface from external environments for days. Controlling the stability of such an instrumental quality of hydrogels determines the service life of soft sensors based on these aqueous entities [55, 56].

2.4 Shape Fidelity and Complex Geometries

The fabrication of conductive hydrogels in three-dimensional shapes has been shown to extend their functionality beyond simple mechanical sensing behavior. Additive manufacturing has been adopted for producing both pure hydrogels and polymer-hydrogel hybrid devices with more versatile, geometrically complex structures, but not all kinds of hydrogel compositions meet the standard qualifications demanded by the particular working mechanisms of commercial 3D printers [57].

Throughout the years, the required properties for printability of soft materials have been obtained by adding auxiliary components, e.g. nanoclay [58], nanocellulose [59], and graphene oxide [60] to thicken gel solutions, combining multiple hydrogels to improve mechanical properties [61], controlling printing temperature [62] and

engineering custom printer heads that are capable of printing under particular conditions [20]. Nevertheless, most current research in this field demonstrate small-scale hydrogel samples (approximately 5 mm to 15 mm) and aim to tune specific properties of the hydrogels by considering certain parameters. The majority of these studies do not attempt to improve all aspects of the hydrogel properties simultaneously. This approach is due to the interdependent nature of the parameters involved which makes it challenging to achieve optimal performance in all desired properties.

To illustrate the influence of geometry on the mechano-electrical behavior of ionic hydrogels, Yin et al. [63] demonstrate a dual-material soft sensor with 3D printed hydrogel beams sandwiched between two elastomer layers. In their work, they show that the distance between the beams can dictate the sensitivity of the soft sensor to different amounts of pressure. Dynamic hydrogel circuits have been fabricated on a millimeter scale using projection microstereolithography (PμSL) which can be locally degraded and repaired to modify the circuit configurations for multiple functional human interfaces [64]. Still, in most existing research, these hydrogels are constructed in either two dimensions or extremely simple three-dimensional shapes. Some have employed a two-step crosslinking method in which the hydrogel solution first undergoes physical crosslinking before the 3D printing process, and is then photo-crosslinked as a post-treatment to enhance print quality and shape fidelity [65]. For hybrid stretchable materials, a recurring method has been to alternatively switch between two precursors to print combinations of hydrogels and different polymers toward the development of more efficient and feasible gel-based electronic devices [66].

All aforementioned research shows vast development in the design and fabrication of three-dimensional hydrogels, yet a simple method to manufacture geometrically complex hydrogel-based devices regardless of their chemistry and composition is yet to be presented.

In this thesis, some of the most common limitations of hydrogel ionotronic devices are targeted in an attempt to develop a reliable and durable soft sensor for human-centric applications.

As a contribution of this work

- A novel production method is presented for flexible electronics by 3D printing hollow elastomer frames to encase ionic hydrogels and function together.
- It is tested and confirmed that this fabricated hydrogel has higher durability and enhanced water retention abilities.
- Various geometries are designed for the hydrogel-based devices to show that they are sensitive enough to give diverse responses to different motions.

Chapter 3

Methodology

3.1 Introduction

This section describes the approach to fabricating hydrogels in their bare and encased forms, testing their water retention behavior, and examining different methods to encase the hydrogels. To answer the aforementioned research questions, the hydrogel composition was inspired by [47], and later adjusted to better suit specific experiments. In upcoming chapters, the composition and designs will be evaluated based on the amount of protection and structural support the encasements provide for the hydrogels, and whether they influence their mechanosensitivity.

3.2 Materials

All the chemicals were used as received without further purification. Acrylamide (AAm), Acrylic Acid (AA), N,N-methylene-bisacrylamide (MBA), Iron (III) Chloride ($FeCl_3$), 2-hydroxy-4'- (2-hydroxyethoxy)- 2-methylpropiophenone (Irgacure 2959), short-chain chitosan (degree of deacetylation $>$ 75-85%, viscosity 20-300 mPa s for 1% (w/v) in 1% acetic acid solution, and molecular weight = 50-190 kDa) were purchased from Sigma-Aldrich (St. Louis, Missouri, USA). Sodium Chloride (NaCl), i.e., table salt, was purchased from local stores. The concentration of materials composing the hydrogel solution is stated in Table 3.1 (For hydrogels containing $FeCl_3$ instead of NaCl, 1 molar or 2 molar solutions were used which correspond to 1.62 g and 3.24 g, respectively). 1.75 mm water translucent CHEETAH TPU filament was purchased from NinjaTek (Manheim, Pennsylvania, USA).

3.3 Equipment

The equipment used for the fabrication of the samples and devices includes a magnetic stirrer from INTLLAB (Greenwood, Indiana, USA), an Ultrasonic Cleaner from Canada Ultrasonics (Newmarket, Ontario, Canada), a Comgrow Creality 3D Ender 5 3D Printer from Creality3D (Shenzhen, China), an LC-3DPrint Box UV Post-Curing Unit from NextDent (Soesterberg, The Netherlands), a PM18C True RMS Multifunctional Digital Multimeter from Aidbucks (China) and an Arduino Uno Rev3 from Arduino. All chemical silverware and glassware were purchased from Sigma-Aldrich (St. Louis, Missouri, USA).

3.4 Methods of Fabrication

To compare the influence of material composition and the protective elastomer encasements in hindering hydrogel water loss, bare and encased hydrogel samples were prepared. The fabrication methods of both hydrogels and hollow encasements are explained in this section.

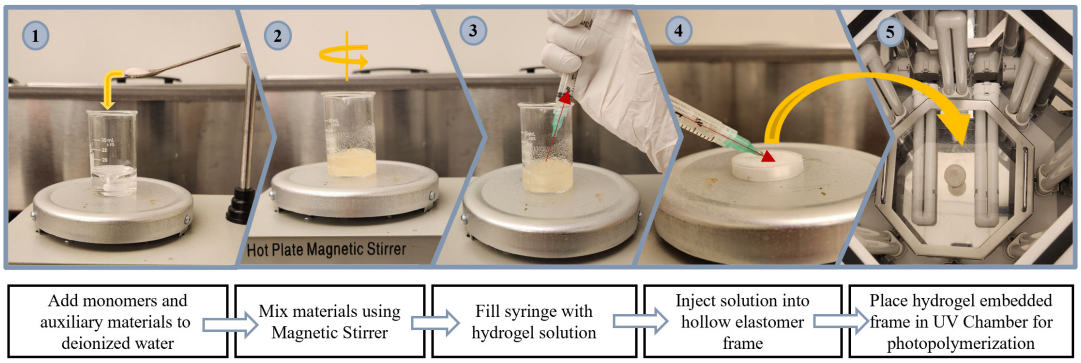

FIGURE 3.1: Fabrication steps of the ionic hydrogel embedded 3D printed elastomer sensor

3.4.1 Ionic Hydrogel Polymerization

The fabrication process of the hybrid sensor is shown in Fig. 3.1. Two different salts ($FeCl_3$ and NaCl) were used to endow the hydrogels with ionic conductivity based on the design and testing situations. For situations in which NaCl was used, the hydrogel was synthesized by firstly mixing AM, MBA as the crosslinking agent, Irgacure 2959 as the photoinitiator, NaCl as an electrolyte, and short-chained chitosan (CS) in 10 mL

TABLE 3.1: Composition of Hydrogel Samples

Sample	Amount
AM	2.2 g
AA	0.33 mL
MBA	4 mg
CS	0 mg – 700 mg
Irgacure 2959	54 mg
NaCl	0.58 g (1 M*) – 1.16 g (2 M)
Deionized Water	10 mL

*M = mol/L

of deionized water, and then gradually adding AA (15% molar ratio of AA/AM) to prevent a sudden increase in viscosity and difficulty in stirring (Steps 1 and 2).

The exact concentration of each component can be found in Table 3.1. The solution was degassed at 50°C for 3 to 5 minutes in an ultrasonic cleaner, depending on the viscosity of the liquid.

To fabricate the bare samples, the solution was then poured into molds and cured under UV light (18 W, 365 nm) in an LC-3DPrint Box. When $FeCl_3$ was used, the hydrogels would be immersed in $FeCl_3$ solution after being solidified (Fig. 3.2). This is because the $FeCl_3$ would inhibit the propagation process and hinder polymerization at early stages, thus its use was avoided in the pre-cure hydrogel solutions.

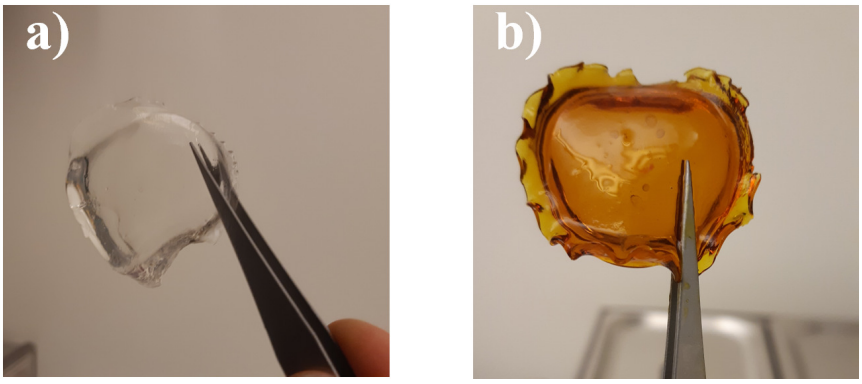

FIGURE 3.2: Cured hydrogel (a) before and (b) after being immersed in 2 M $FeCl_3$ solution for 24 h

3.4.2 3D Printing Elastomer Frames

The hollow elastomer frames were designed in Fusion 360 software. Translucent TPU filament was used to realize the designs using a Creality Ender 5 3D printer while transmitting UV light to allow the photopolymerization of the hydrogel. Additive

manufacturing was done at a print speed of 35 mm/s, 0.1 mm print accuracy, and a temperature of 235°C. After the object was printed, the prepared pre-cure gel solution was gathered into a syringe (Step 3) and injected into the hollow elastomer frame (Step 4). After the hybrid samples were irradiated under UV light (Step 5), they were connected to an Arduino Uno setup to be tested for mechanical sensing.

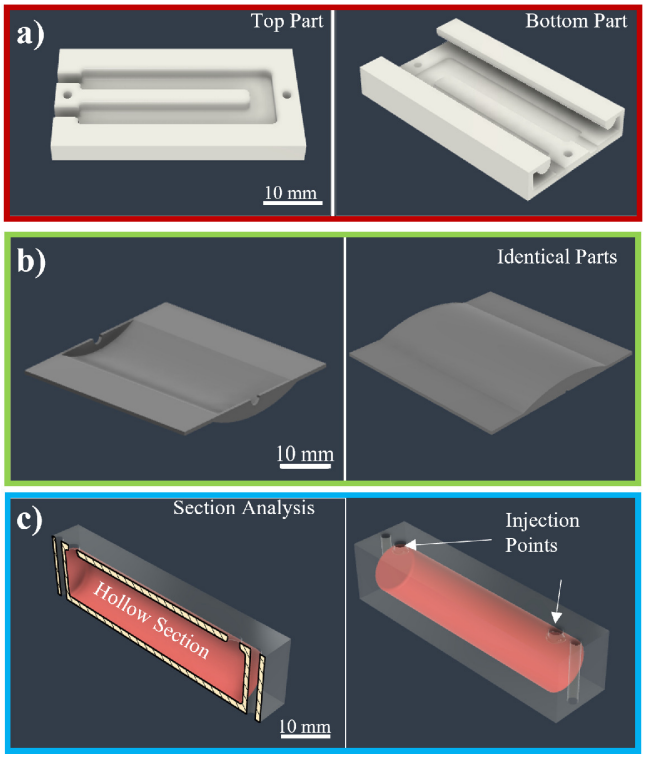

FIGURE 3.3: CAD designs of a) the two-component snap-fit encasement b) identical two-component double-sided encasement and c) a half-section analysis and full view of the injectable encasement

3.4.3 Encasement Methods

Several techniques to embed hydrogels into elastomer frames were employed to create sensors with more complex geometries. As shown in Fig. 3.3, these designs consisted of

a. Two snap-fitting components meant to be embedded with hydrogel on one side

b. Two identical components meant to both be embedded with hydrogel and assembled using clamps

c. A single hollow component meant to be embedded with hydrogel via injection with no need for assembly

3.5 Characterization

3.5.1 Water Retention

The water retention ability of bare and encased hydrogels with various compositions was assessed by repeatedly recording their weight at different times. The change in water content was reported in terms of the percentage of weight lost:

$$\Delta W = \frac{W_0 - W}{W_0} \times 100, \tag{3.1}$$

where W is the weight of the water remaining in the hydrogel at each time, and W_0 is the weight of initial water content at $t = 0$.

3.5.2 Mechanical Sensing

Aside from the changes in electrical resistance induced by the altered orientation of hydrogel chain entanglement, the macroscopic changes in the hydrogel dimensions would also affect its electrical properties.

The electrical resistance of any material follows Pouillet's law of resistivity:

$$R = \rho \frac{l}{A}, \tag{3.2}$$

where ρ is the resistivity (which relies solely on the material properties in various external conditions), l is the sample length, and A its cross-section, indicating that the resistance of an object is dependent on its dimensions, and therefore directly affected by deformation.

To assess the dependence of their electrical properties on mechanical stimuli, the change in resistance of the ionic hydrogels was observed and calculated by

$$\Delta R = \frac{R - R_0}{R_0} \times 100, \tag{3.3}$$

where R is the resistance at each moment, and R_0 is the initial resistance of the sample. An Arduino Uno ohmmeter was used to measure resistance change under different amounts of mechanical loading. The response of the ionic hydrogel to pulling, pressing and bending was tested.

Chapter 4

Water Retention, Shape Fidelity, and Mechanosensitivity

4.1 Introduction

To test for water retention properties and mechanosensitivity, acrylamide-based hydrogels were fabricated with fixed concentrations of auxiliary materials, which were adjusted as necessary to achieve desired properties. As a hydrophilic polymer, polyacrylamide has good water absorption but relatively low mechanical properties and insufficient hydrolytic stability, meaning that they undergo hydrolysis when immersed in water and their structure breaks down. The copolymerization of acrylamide with acrylic acid confers ion exchange properties on the hydrogel as well as increasing its water retention ability and tensile strength. Additionally, crosslinking the copolymer with MBA through a vinyl addition polymerization results in a gel with varying porosities depending on the concentration of the crosslinker and monomers, and polymerization conditions [67]. To examine the impact of chitosan, various hydrogel samples were created with varying amounts of the substance. The samples were then tested to determine how chitosan affected their injectibility into elastomer frames and water retention behavior in both bare and TPU-encased hydrogels. The ionic hydrogels demonstrated satisfactory mechanosensitivity, and hybrid elastomer/hydrogel designs were shown to display distinguishable signals under different types of mechanical stimuli.

TABLE 4.1: Composition of Hydrogel samples to compare for water retention

Sample	**Chitosan**	**TPU**
PAAm	×	×
450-CS-PAAm	$450mg$	×
700-CS-PAAm	$700g$	×
Hybrid	×	YES
450-CS-Hybrid	$450mg$	YES

4.2 Water Loss in Bare and Encased Hydrogels

As shown in Table 4.1, three polyacrylamide (PAAm) based samples were generated, two of which contained different amounts of chitosan (CS) (labeled PAAm, 450-CS-PAAm and 700-CS-PAAm). The Hybrid and 450-CS-Hybrid samples consisted of hydrogel-embedded disk-like TPU frames to mimic the shape of the bare hydrogels cured in Petri dishes. After fabrication, all the samples were left to air dry in the same ambient conditions for up to 60 hours to compare the influence of Chitosan and 3D printed encasements on their water retention ability.

Initial water content was calculated to be approximately 80 w% for all bare and encased samples based on the ratio of deionized water to the total materials used to prepare the pre-cure polymer solution. It is seen in Fig. 4.1c that chitosan content contributes to maintaining water within the polymer chains of the ionic hydrogel. This effect is possibly due to the extra crosslinks that the chitosan molecules create with the main polymer chains consisting of AAm and AA. With an increase in the number of crosslinks within the hydrogel structure, the free volume formed between the polymer chain is divided into smaller sections. Following the decrease in the pore size, water molecules are better entrapped within the chains, which hinders their evaporation from the polymer structure. The hydrophilic functional groups comprising the Chitosan structure could also create hydrogen bonds as well as Van der Waals bonds with the water molecules, further entrapping them within the hydrogel pores.

Accordingly, the results of the water retention tests displayed in Fig. 4.1c show chitosan content had a positive effect on the water retention ability of the hydrogels, although small. While 60% of the PAAm sample's initial water content evaporated in under 15 hours, 700-CS-PAAm lost 54%, on average. Within 60 hours, the results remained consistent as PAAm, 450-CS-PAAm and 700-CS-PAAm lost 85.5%, 81.8%

and 78.2% of their water, respectively. After losing most of their water content, the samples no longer maintained their gel-related behavior and acted as brittle non-aqueous polymers. Considering the minimal contribution of chitosan to the water retention abilities of the hydrogels, this rate of water loss within a small time frame necessitated a different approach to ensure the durability of the hydrogel's mechanical and electrical behavior. This issue was addressed by the fabrication of elastomer encasements for the hydrogels through extrusion 3D printing.

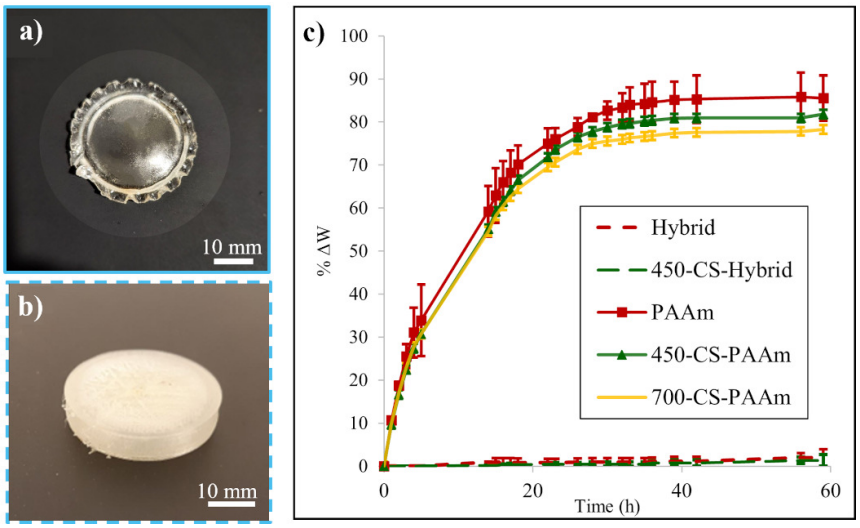

FIGURE 4.1: (a) Bare ionic hydrogel and (b) hydrogel embedded TPU frame (c) Water loss (w%) of bare and encased hydrogel samples with different chitosan content within 60 hours

Hollow TPU frames were fabricated to fully cover the hydrogels and protect them from the external environment, and further improve their water retention. To evaluate the efficacy of this method, cylindrical TPU disks (illustrated in Fig. 4.1b) were fabricated to mimic the exact shape and dimensions of the polymerized bare hydrogels (Fig. 4.1a). The frames were injected with pre-cure hydrogel solution which was then solidified under UV irradiation. It is clearly observed in Fig. 4.1c that the protective encasements were highly effective in obstructing water evaporation from the hydrogel surface. While 80% of the water content of PAAm and 450-CS-PAAm evaporated after 30 hours, the Hybrid and 450-CS-Hybrid samples lost only 1.9% and 1.3% after 60 hours, respectively. Although chitosan content in both hybrid samples seemed insignificant in the matter of water retention, it contributed in terms of injectibility and compatibility with the elastomer surface. The more viscose 450-CS-PAAm was injected into the frame more conveniently, spreading out uniformly into the empty

space without forming any air bubbles. After polymerization, even though both encased hydrogels showed higher durability in water-related properties, 450-CS-Hybrid exhibited more structural stability as the hydrogel from the Hybrid sample dislodged from the inner TPU layer and left air cavities inside the printed cylinder within 24 hours. This is possibly due to a larger mismatch between the hydrogel and TPU polymer in the Hybrid sample compared to 450-CS-Hybrid. The chitosan content increased the number of crosslinks within the polymer chains resulting in higher toughness and Modulus of the hydrogel, which brought it closer to the mechanical properties of the TPU elastomer frame. The dislodged location and area could vary case by case, and unpredictably compromise the structural and electrical behavior of the sample. Based on these results, 450-CS-Hybrid was chosen to be used in the following experiments regarding the complex geometry hybrid sensors.

4.3 Sensing Abilities of Bare and Encased Hydrogels

To set up a baseline, bare ionic hydrogels were fabricated to be evaluated for sensitivity to mechanical loading. The tests were done immediately after the samples were cured to eliminate the effects of water loss on sensitivity as much as possible.

Figure 4.2a demonstrates the response of two ionic hydrogel samples with different NaCl concentrations to static pressure. The signals had oscillations within the plateau but were easily distinguishable from when the hydrogels were left untouched. These oscillations may have been due to variations in static pressure, or unintended movements of the metal electrodes. This could be the cause for the drop in overall resistance as well. Another possible explanation for the change in the absolute resistance is that when the external source of pressure was removed from the ionic hydrogel, the residual stress formed in the hydrogels during fabrication was released. This phenomenon might have led to the continual movement of the polymer chains relative to each other, which changed the paths that permit ion transfer.

The sample containing 2 M NaCl was used to test if the hydrogel would be able to discern different amounts of pressure. It can be observed from Fig. 4.2b that the resistance of the conductive hydrogel initially decreased by 29% when pressed lightly, and 43% when pressed heavily. Fig. 4.2c shows that the ionic hydrogels containing

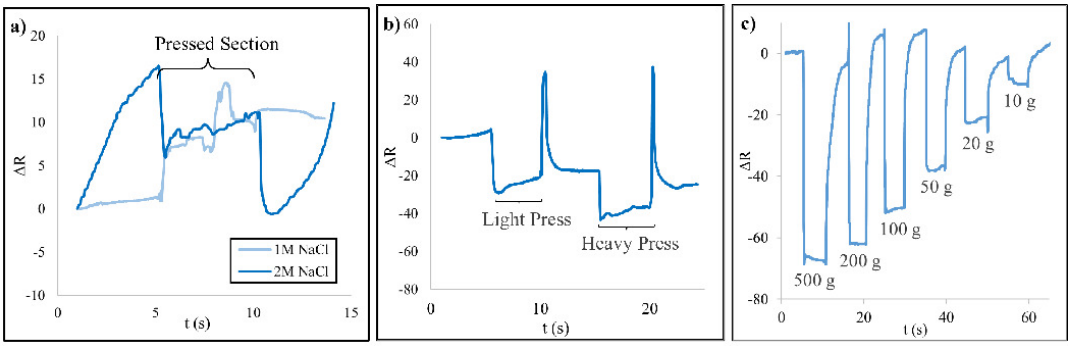

FIGURE 4.2: (a) Response of bare 1 M and 2 M NaCl hydrogel samples to pressure (b) response of bare 2 M NaCl hydrogel sample to light and heavy pressing and (c) response of 2 M bare $FeCl_3$ hydrogel samples to loading under different weights

$FeCl_3$ were also able to detect different amounts of pressure through changes in their resistance proportional to the weight of the object placed on top of them (10 g, 20 g, 50 g, 100 g, 200 g, and 500 g). This difference in responsivity implies that the electrical resistance of the hydrogel was sensitive to the extent of deformation. The more the hydrogel structure deformed and caused variations in ion migration paths, the more vastly its ionic conductance was altered.

Chapter 5

Complex Geometry and Electro-mechanical Behavior

3D printing brings forth the possibility of creating ionic hydrogel sensors in various shapes and sizes, in contrast to their more common thin-film form. After demonstrating the electrical sensitivity of bare ionic hydrogels to mechanical loading, 450-CS-PAAm samples containing 2 M NaCl were injected into 3D printed TPU frames for higher geometric complexity, better water retention, and to eventually be able to control the direction of hydrogel deformation for mechanical sensing. After determining the most effective method of hydrogel encasement between the snap-fit, double-sided and injectable designs, basic hybrid sensors were designed and printed to examine the response of the hybrid elastomer/hydrogel sensors to pressing, pulling, and bending based on the type of deformation that their designed geometry allowed. These geometries included a dogbone, a strain gauge, and a finger-shaped cylinder.

5.1 Design approaches to Elastomer Encasements

5.1.1 Snap-fit Encasement Design

The 3D printed top and bottom snap-fitting components are shown in Fig. 5.1a. These components are assembled as demonstrated in Fig. 5.1b. Because of the relatively lower print resolution of flexible materials due to their low elastic modulus, it was difficult to design and accurately print to snap-fitting parts that fit together seamlessly. This factor added into the already existing gaps within assembled components left room for the water to evaporate from the hydrogel —not as rapidly as the

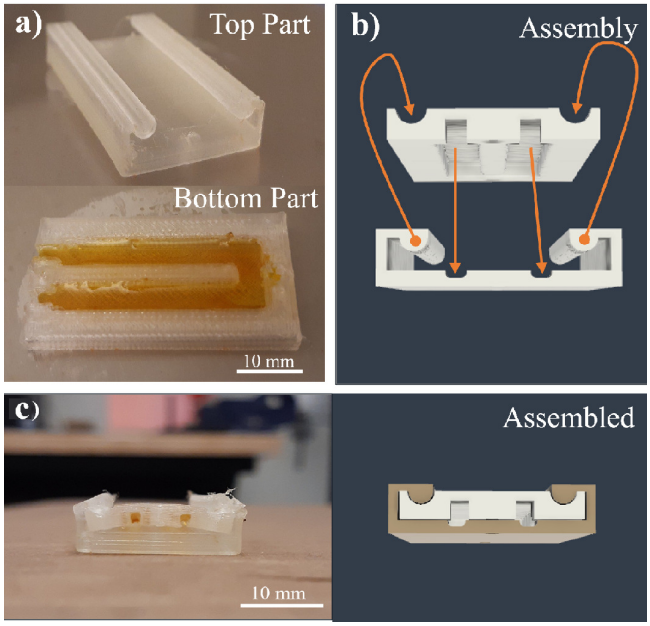

FIGURE 5.1: (a) Top and bottom components of the snap-fit design, (b) schematics of how they fit together and (c) the warped shape of the assembled sample in comparison to its CAD model as a result of water evaporation from the hydrogel

bare samples— but still within a few days. When the hydrogels dried, they decreased in volume while still bound to an elastomer component, causing the parts to deform from the shape it was designed to create (Fig. 5.1c). So, even if this type of encasement did allow for the ionic hydrogels to detect deformation through changes in their electrical behavior, it was not a suitable candidate to extend its water retention and structural durability.

5.1.2 Double-Sided Encasement Design

The double-sided design consisted of two identical substrates with space for the hydrogel to be embedded. After the hydrogel was cured on both substrates, they were held together by alligator clamps, two pairs were used for keeping the sensor together, and a pair was used as the electrodes. As shown in Fig. 5.2, this design showed high amounts of pressure-sensing (up to 500% resistance change according to Fig. 5.2a). Still, quite similarly to the snap-fit design, there were gaps at the interface of the two components, exposing the hydrogels to the external environment and allowing for high amounts of water loss. Another complication of this approach was that the merest change in clamp orientation when assembling the components would modify

the pattern of resistance change, which compromised the reliability of the signals.

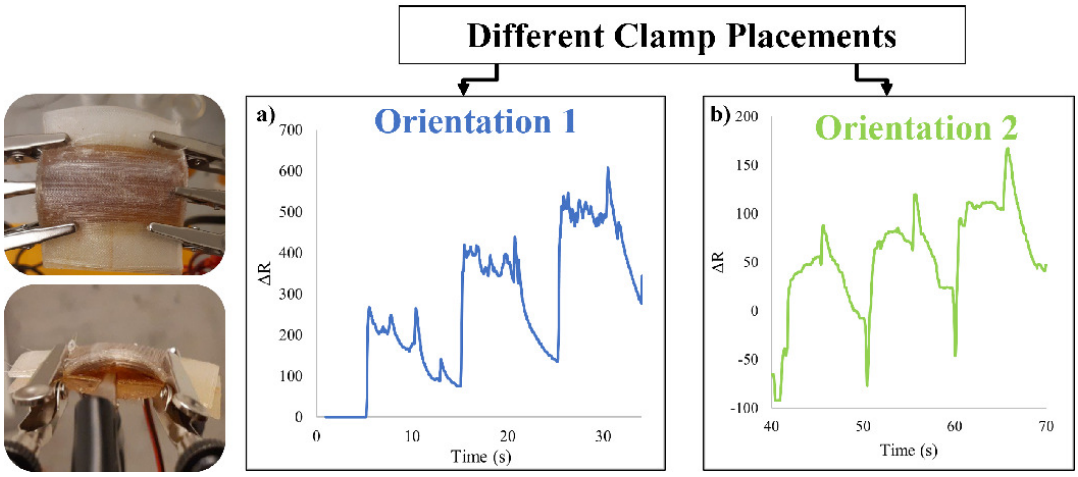

FIGURE 5.2: Varying patterns of resistance change relying clamp and electrode placement

5.1.3 Injectable Design

In contrast to the first two approaches to designing protective encasements for hydrogels, the injectable design was comprised of only one component, with small holes which enabled injection of the ionic hydrogel into its internal hollow space. This design was tested for sensitivity to pressing and pulling, and only responded to the former, due to the types of deformation that its geometry allowed (Fig. 5.3).

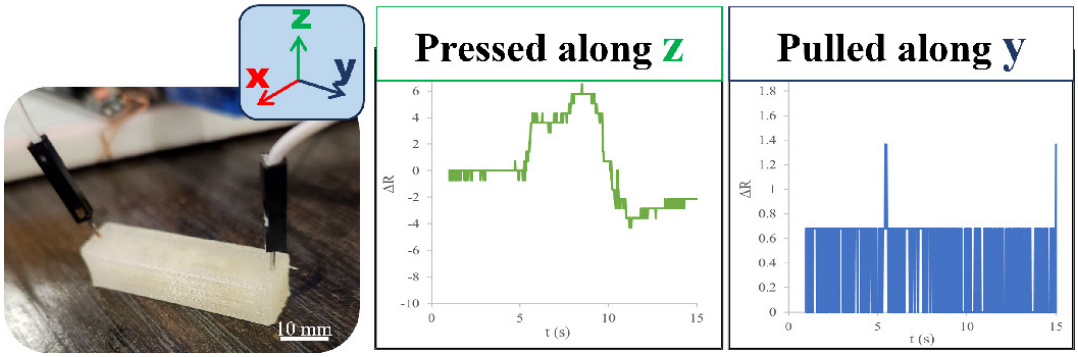

FIGURE 5.3: Response of the injectable design to pressing and pulling

Since the rectangular cube was not flexible enough in the direction of its length, the hydrogel was not deformed and therefore its resistance did not change. It is important to note that for this experiment, it was attempted to include $FeCl_3$ salt by filling half the volume of the encasement cavity with hydrogel solution, and the other half with $FeCl_3$ solution after removing the hybrid sensor from the UV chamber,

since this salt could not have been used in the pre-cure solution. In this way, the solidified hydrogel would absorb the salt within the encasement structure —ideally in a uniform distribution— and become ionically conductive. This method was later discarded due to difficulty in implementation, non-uniform absorption, and unreliable electrical response of the hybrid structure and $FeCl_3$ was replaced with NaCl.

5.2 The Influence of Geometry on Mechanosensitivity

5.2.1 Dogbone

The small dogbone object was designed with a cylindrical cavity to hold the hydrogel as shown in Fig. 5.4a. After curing, its response to pressing and bending was observed by inserting electrodes into its sides. It is demonstrated in Fig. 5.4b that the hybrid dogbone sensor responded with distinguishable signals when it was pressed lightly (∼0.5 N) and heavily (∼1 N) in the middle. The light press elicited a smaller increase in the resistance, up to 7.4%, while the heavy press caused an up to 8.6% increase in resistance. Additionally, Fig. 5.4c shows that bending the sensor at small and large angles was followed by resistance change corresponding to the bending angle.

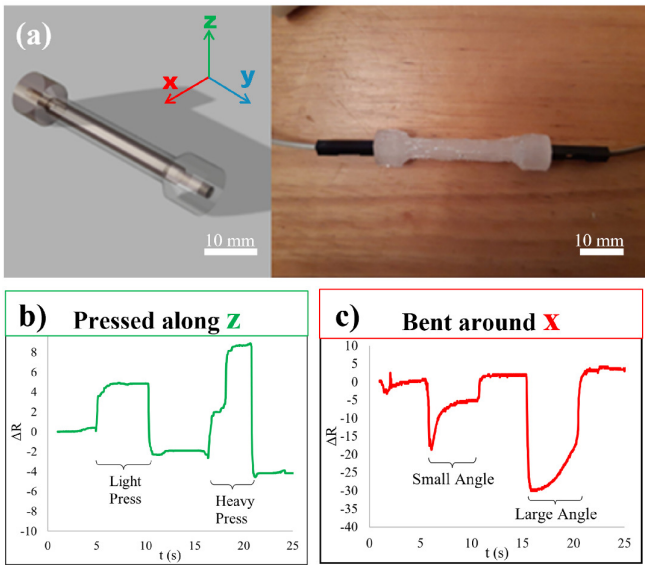

FIGURE 5.4: (a) CAD design and printed dogbone sensor (b) response of the dogbone sensor to light and heavy pressure and (c) small and large bending angles about its length.

The section for large-angle bending shows a curve before returning to initial resistance which can be due to the gradual relaxation of the hybrid dogbone to its original

shape. Some random signal peaks and inconsistencies also seen in the plots were attributed to the movement of the electrodes within the soft sensor.

5.2.2 Strain Gauge

The strain gauge shown in Fig. 5.5a was injected with ionic hydrogel and evaluated for a response when pulled from both sides. In contrast to the dogbone, electrodes were inserted into the strain gauge pre-cure so that they would be entirely covered by the hydrogel after polymerization to diminish irrelevant signals. The strain gauge shown in Fig. 5.5a was tested for response to mechanical loading by pulling the object from both sides. Fig. 5.5b demonstrates the response of the hybrid sensor in terms of resistance change. Small rises in resistance are observed in response to three consecutive cycles of pulling, which is due to the lengthening of the path through which the ions transfer. The relatively noisy electrical response possibly occurred because the object design was too long for the ions to efficiently transfer charge from one side of the circuit to the other. It was also likely that the design geometry did not properly accommodate expansion in the pulling direction, leaving little room for deformation.

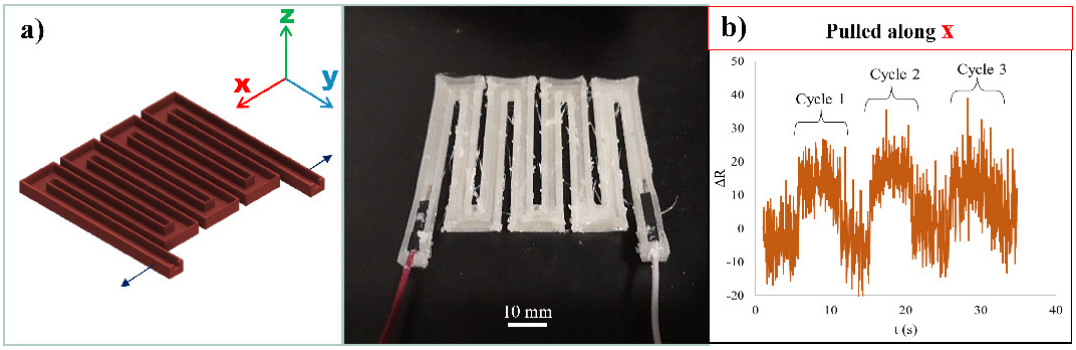

FIGURE 5.5: (a) CAD design and printed strain gauge (b) response of the strain gauge sensor to being pulled from both sides

5.2.3 Finger-shaped Cylinder

The design and print of the finger-shaped cylinder are shown in Fig. 5.6a. The cylinder was designed with a U-shaped cavity to hold the hydrogel. Figure 5.6b shows that the finger-shaped sensor was able to detect pressure both in the middle, at the bottom, and the tip. While the response to pressing the middle and the bottom of the cylinder

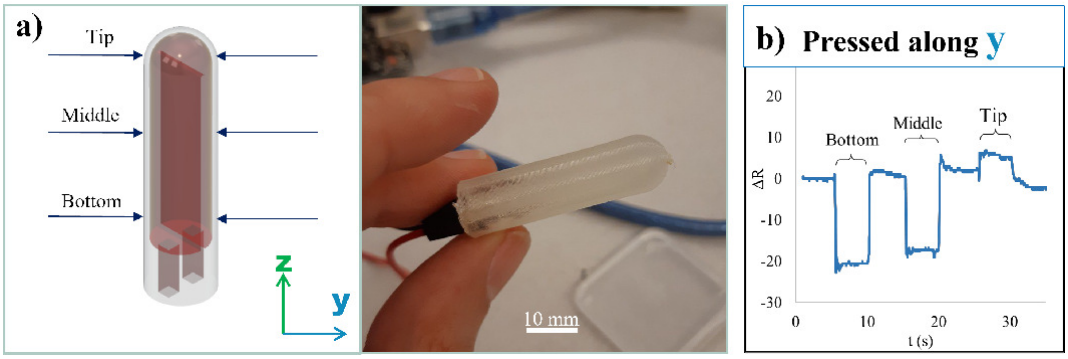

FIGURE 5.6: (a) CAD design and printed finger-shaped object (b) response of the finger-shaped sensor to being pressed in the middle, at the bottom, and the tip

was exhibited as drops in the resistance, pressing the tip led to a smaller and positive percentage of resistance change.

As the final basic hybrid design, a finger-shaped cylinder was designed with a U-shaped cavity to hold the hydrogel (Fig. 5.6a). For this sensor, two cubic spaces were also designed at the bottom where the electrodes would be inserted to fasten the electrodes in the device and reduce their movement and eliminate sudden peaks in the signal. The resistance change plot in Fig. 5.6b depicts how the sensor recognized pressure at different locations of the object. At the bottom and middle of the sensor, the resistance dropped around 20% and 16% respectively in response to pressure, indicating analogous sensitivity. In contrast, when the sensor was pressed at the tip, it increased by around 6%. This discrepancy could be attributed to the difference in hydrogel geometry within the particular design. At the bottom and the middle, the hydrogel was deformed in two sections of its length separated by a 0.8 mm thin. The response suggests the potential for charge to pass through the thin wall when pressed, creating shorter routes for ion transfer. The sensing mechanism at the tip was different due to the continuous mass of hydrogel cured at the bottom of the “U" of the U-shaped cavity, lacking the thin partition. This variation in geometry dictated the deformation in the hydrogels following mechanical loading, which affected their electrical response at different locations.

5.2.4 Glove-shaped Sensor 1

After observing the response of the hybrid sensor to pressing, pulling and bending, more complex objects were 3D printed to confine the ionic hydrogel. Firstly, a three-finger glove suited to fit the index, ring and middle fingers of the human hand was printed, illustrated in Fig. 5.7a. The design consisted of a main body to cover the fingers, and a bridge to connect them to accommodate both bending and stretching apart.

As demonstrated in Fig. 5.7b, rises in the hydrogel resistance can be seen following three consecutive cycles of bending all three fingers simultaneously, which is ascribed to both the inward bending of the frame and the outward pressure exerted onto the object from the back of the knuckles. Furthermore, the sensor also responded when the fingers were stretched apart from each other by a decrease in resistance in three consecutive turns through the lengthening of the bridge components (Fig. 5.7c).

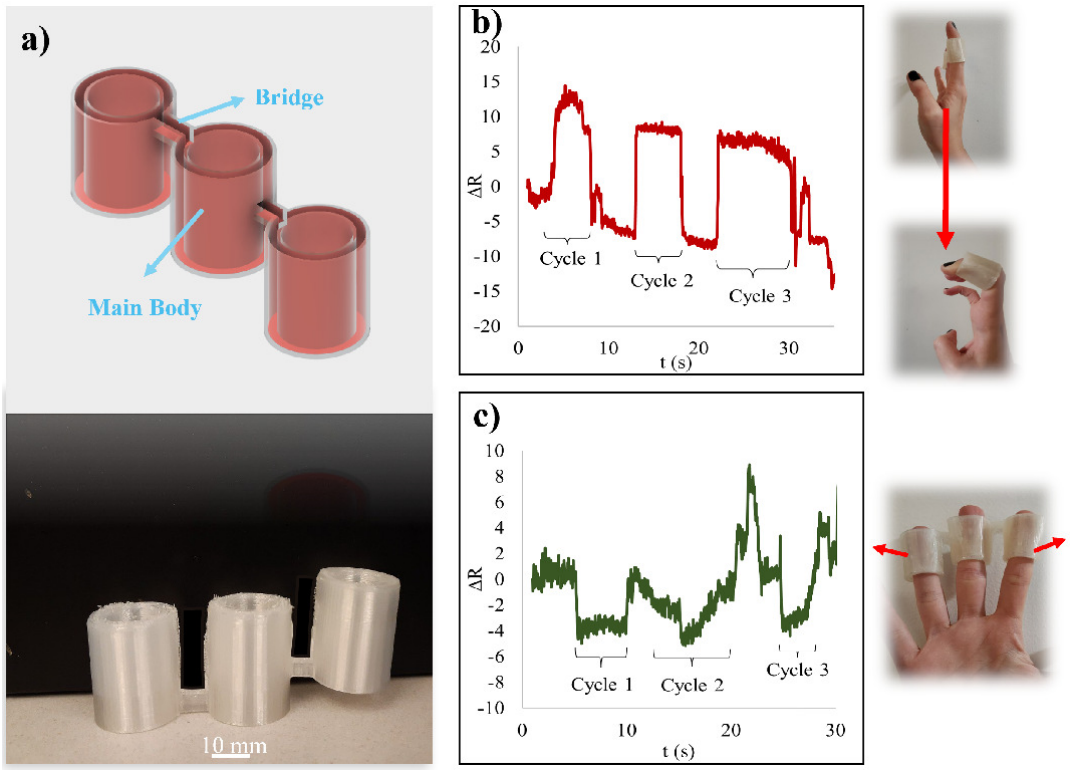

FIGURE 5.7: (a) CAD design and printed glove-shaped sensor 1, (b) its response to bending fingers and (c) stretching fingers apart for three cycles.

Python code was used to detect and differentiate between bending the fingers and stretching them apart on the hybrid glove mechanical sensors. The pseudocode of the

finger motion detection program can be seen in Algorithm 1.

Even though the hydrogel was able to respond well while confined in this geometry, the straight design of the bridges allowed for little extension, and the large surface area of the wearable sensor complicated the free and independent movement of the individual fingers. As a solution, a lighter, less constricting wearable sensor was designed, as shown in Fig. 5.8a.

ALGORITHM 1: Finger Motion Detection

```
Read the CSV file of the sensor response into Dataframe
Convert Dataframe to array 'data' with columns 't' and 'R'
bendSignal ← Bend Signal Threshold
tResponse ← 40 iterations
pullSignal ← Pull Signal Threshold
pullEdge ← 1 and bendEdge ← −1
for length of time series i do
    deltaR ← data[i + tResponse][R] − data[i][R]
    if deltaR < pullSignal then
        if next iteration > pullSignal then
            pullEdgeOld ← pullEdge
            pullEdge ← deltaR
        end
        if pullEdge × pullEdgeOld < 0 then
            Print 'Stretching at data[i][t]'
        end
    end
    if deltaR > -pullSignal then
        if next iteration < pullSignal then
            pullEdgeOld ← pullEdge
            pullEdge ← deltaR
        end
        if pullEdge × pullEdgeOld < 0 then
            Print 'End of stretching at data[i][t]'
        end
    end
    if deltaR < bendSignal then
        if next iteration > bendSignal then
            bendEdgeOld ← bendEdge
            bendEdge ← deltaR
        end
        if bendEdge × bendEdgeOld < 0 then
            Print 'Bending at data[i][t]'
        end
    end
    if deltaR > -bendSignal then
        if next iteration < bendSignal then
            bendEdgeOld ← bendEdge
            bendEdge ← deltaR
        end
        if bendEdge × bendEdgeOld < 0 then
            Print 'End of bending at data[i][t]'
        end
    end
end
```

5.2.5 Glove-shaped Sensor 2

A lighter glove design with empty spaces in front of the knuckles was designed for more freedom of movement (Fig. 5.8a). The bridges which held the main body together were shaped into half moons to accommodate horizontal extension. This glove was also designed with space for the electrodes to be inserted into the pre-cure gel solution for better mechanical and electrical stability of the entire system.

Figs. 5.8b and 5.8c depict the response of the lighter glove-shaped sensor to stretching the index and middle fingers, and the middle and ring fingers in arbitrary units of resistance, respectively. Additionally, when the index, middle and ring fingers were bent down one by one, the wearable sensor responded with changes in its resistance, as shown in Figs. 5.8d, 5.8e, and 5.8f, respectively. The plots show significant drops in resistance as a result of bending the index and ring fingers, but smaller rises in resistance following the bending of the middle finger. This could be because the middle part of the glove was surrounded by two bridges and could hold less amount of conductive hydrogel in the empty space. Nevertheless, this design enabled relatively free and independent movement of all three fingers in more than one direction and was able to detect those movements through changes in the electrical signal.

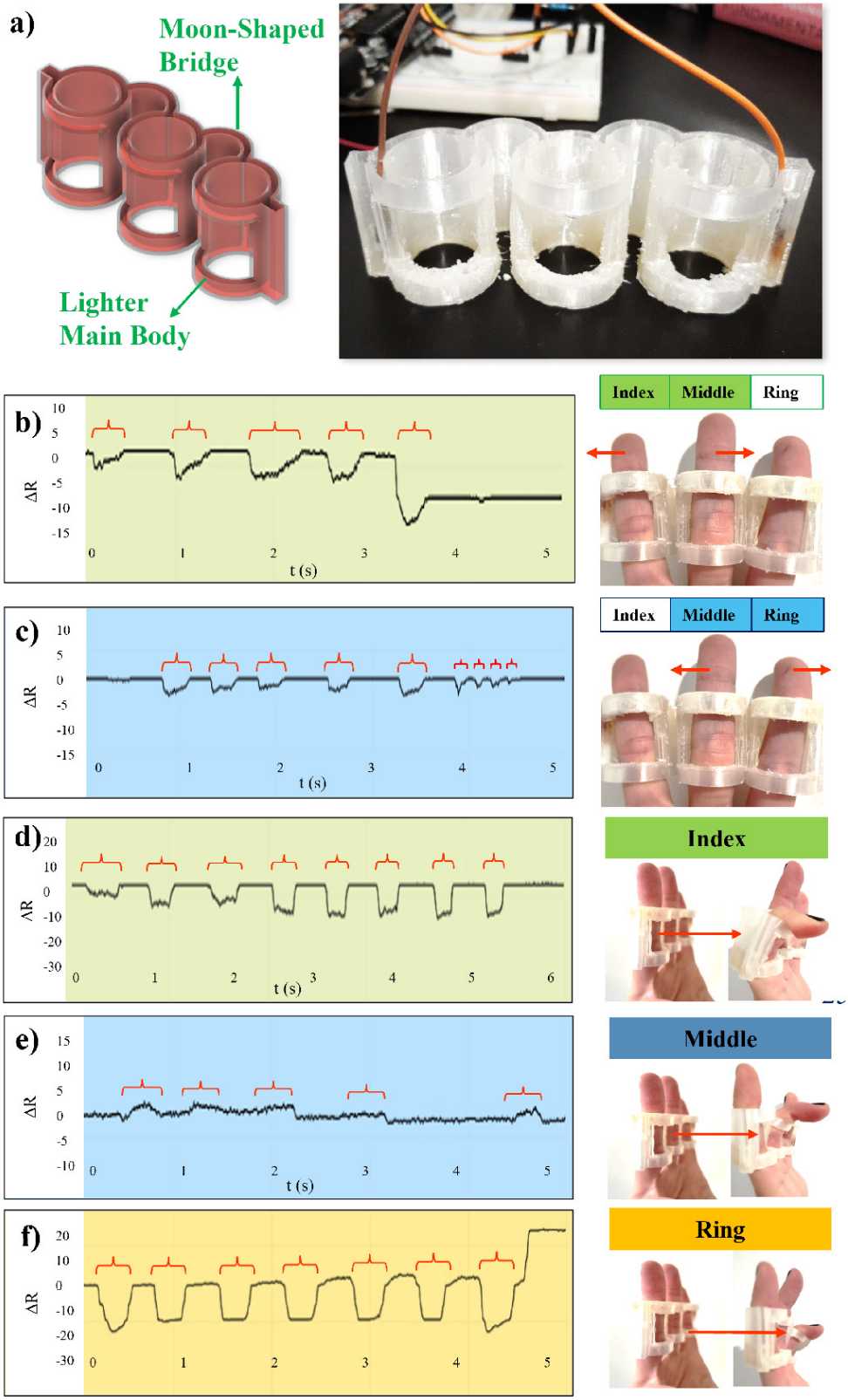

FIGURE 5.8: (a) CAD design and printed glove-shaped sensor 2 and its response to (b) stretching apart Index and Middle fingers, (c) stretching apart Middle and Ring fingers, (d) bending Index finger, (e) bending Middle finger, and (f) bending Ring finger. (Sections of the graphs that are marked with accolade symbols show the ranges in which the sensor was stimulated)

Chapter 6

Discussion

This research demonstrates that given the appropriate geometry, the hybrid hydrogel sensors responded to mechanical loading similarly to the bare ionic hydrogels, albeit with generally lower sensitivity due to the constriction of their deformability by the TPU elastomer. They also exhibited significantly lower rates of water evaporation than the bare hydrogels that were directly exposed to air, which faced issues in maintaining their electrical conductivity as well as their gel-related properties. The 3D printed TPU frames acted as encasements to cover the outer surface of the ionic hydrogels and protect them from water evaporation. Additionally, they enabled the design and fabrication of complex application-defined hollow geometries to counter the low mechanical stiffness of the aqueous hydrogel structures that reduces their shape fidelity at larger scales. These hybrid objects could be designed in specific shapes to accommodate the detection of mechanical stimuli in different forms and directions without the need to carry out laborious assembly steps.

Comparing the results from electrical tests on the bare (Fig. 4.2) and encased ionic hydrogels (e.g., Fig. 5.5), it becomes clear that the bare hydrogels and the hybrid samples have similar sensitivity, i.e., they both have similar changes in resistance, around 10-60%. This means that although the lower flexibility of the TPU elastomer increases the elastic modulus of the hybrid system, it does not significantly affect the hydrogel performance. Also, there are sudden large peaks and changes in absolute resistance seen at the end of the response signal in the bare hydrogel after the pressure is removed from the sample. These irregularities are most probably caused by movements in the electrodes, changing their contact area with the conductive hydrogel. Conversely, there are no such peaks seen in the resistance change of the hybrid

samples, where electrodes were fixed in solidified hydrogel and in-between robust elastomer walls. This effect is especially reduced in designs such as the finger-shaped object (Fig. 5.6) and the second glove design (Fig. 5.8) where there were designated slots designed for the jump wires to be inserted.

We observe that the signals in the strain gauge sample in Fig. 5.5 have much more fluctuations than other examples. This is not a result of the hydrogel being encased, since the hybrid dogbone and cylinder samples in Figs. 5.4 and 5.6 show stable responses. The difference between them is the travel length of the ions. The sinuous strain gauge has a much longer travel length, which results in more noise and instability. However, the change in resistance to mechanical stimuli is still prominent.

Sharp edges may also negatively affect the smoothness of the signals. The appropriate length and cross-section of the glove designs in Figs. 5.7 and 5.8 allowed them to acquire detectable resistance change from the movement of fingers, following the same deductions. Therefore, the mechano-electrical properties of the hydrogel-based sensors were considerably influenced by various geometrical parameters in addition to their chemical composition.

In general, the complex geometry of the elastomer/hydrogel sensors made it difficult to analyze the reasons behind the patterns of resistance change, due to the multifarious parameters affecting the deformation and conductance of the hydrogels. For example, as a result of bending fingers, while wearing the glove designs, different parts of the design would be under tension or compression in various directions based on their placement on the hand, making it quite difficult to track the dominant mechanism controlling the electrical behavior and resistance change pattern of the hybrid sensor.

Ultimately, when considering the response patterns in all of the diverse designs demonstrated for the hybrid ionic sensors, it is clear that geometry played a significant role in determining the type and direction of mechanical loading, as well as the variation in electrical signals when the conductive component of the devices was deformed. For instance, the dogbone design did not permit high amounts of strain to be exerted onto it along its length but was easily pressed and bent to obtain a significant electrical response (Figs. 5.4b and 5.4c, respectively). In contrast, the thin zig-zag shape of the strain gauge was not suitable to sense bending or pressure but had a

response to being pulled from both sides. The more complex glove-shaped sensors (Figs. 5.7 and 5.8) accommodated movement and sensing in two directions. While the bridge sections of the design responded to the fingers being stretched apart from each other, the main body of the glove was able to detect the bending of the fingers. The significance of sensor geometry can once again be observed in the response of the second glove-shaped sensor, where the plots in Fig. 5.8 demonstrate its ability to detect independent bending and stretching of the fingers due to the less constricting main body, and more deformable circular bridges.

Tactile perception is one of the main functions that help human beings to perceive the external environment. These durable, robust hybrid sensors can be employed as medical prosthetic devices, sensors for healthcare monitoring, and human-robot interactions. Specifically, the glove-shaped sensors could be used for monitoring in physical therapy and rehabilitation, be it as a wearable or a conductive prosthetic device. Their ability to detect hand gestures and independent finger movements creates opportunities to translate the signals into meaningful outputs, such as musical notes, interpreting sign language, or commands for remote control. The possibility to customize designs and print hollow frames in desired geometries grants the vast potential for a wider range of alternative applications for these hybrid elastomer/hydrogel sensors.

Chapter 7

Conclusion

A series of hybrid elastomer/hydrogel devices were demonstrated as ionic mechanical sensors. The electronic devices consisted of an ionic conductive hydrogel component that was injected into various 3D printed geometries to provide the hydrogel with protection from the external environment and enable the fabrication of complex three-dimensional geometries. The injected hydrogels were then cured under UV irradiation. Then, the hybrid devices were tested under pressing, pulling, and bending for mechanical sensing functionality. As a result of deformation in the hydrogel structure, these ionic sensors were able to detect different types of mechanical loading through changes in resistance correlating to the amount of force exerted onto them. Moreover, hybrid wearable sensors were also designed and 3D printed. The hydrogel-embedded gloves were able to detect when the fingers were bent and stretched apart from each other. While taking into consideration the significance of hydrogel deformation and water retention, this thesis explores the potential of these hollow frames to be designed in various geometries for hydrogel encasement to fit a range of specific applications in human-machine interfaces, soft robotics, and personal healthcare monitoring.

The hybrid sensing system presented in this thesis showed promise as a stretchable ionic sensor responding to different mechanical stimuli. Nevertheless, there is much room for improvement in its fabrication steps and operation. The relatively low sensitivity of the hybrid device due to its high resistance could be enhanced using stronger salts as the electrolyte and more suitable geometries for the body and cavities of the elastomer frame. Although the high durability of the hydrogel-embedded elastomers was demonstrated in terms of high water retention, cyclic stability of electrical properties and signal consistency could also be examined in the future. Furthermore,

investigating the exact correlation between different geometrical features of the design and the electrical response could be useful in figuring out the best approaches to designing the 3D printed sensor for amplified response to mechanical loading. Elastomer filaments with varying elastic moduli can be used as hydrogel encasements to reduce the mismatch between elastomer and hydrogel mechanical properties. The effect of different elastomer frames on the hybrid sensor performance and workability could also be examined in future works.

Bibliography

[1] Manwen Zhang, Xinglin Tao, Ran Yu, Yangyang He, Xinpan Li, Xiangyu Chen, and Wei Huang. Self-healing, mechanically robust, 3D printable ionogel for highly sensitive and long-term reliable ionotronics. *Journal of Materials Chemistry A*, 10:12005–12015, 2022.

[2] Chiyu Fu, Kai Wang, Wenyang Tang, Azadeh Nilghaz, Christopher Hurren, Xungai Wang, Weilin Xu, Bin Su, and Zhigang Xia. Multi-sensorized pneumatic artificial muscle yarns. *Chemical Engineering Journal*, 446:137241, 2022.

[3] Wenlian Qiu, Changgeng Zhang, Guoqing Chen, He Zhu, Qi Zhang, and Shiping Zhu. Colorimetric ionic organohydrogels mimicking human skin for mechanical stimuli sensing and injury visualization. *ACS Applied Materials & Interfaces*, 13(22):26490–26497, 2021.

[4] Kenneth D. Harris, Anastasia L. Elias, and Hyun-Jong Chung. Flexible electronics under strain: A review of mechanical characterization and durability enhancement strategies. *Journal of Materials Science*, 51(6):2771–2805, 2015.

[5] Mu Shik Jhon and Joseph D. Andrade. Water and hydrogels. *Journal of Biomedical Materials Research*, 7(6):509–522, 1973.

[6] Buddy D. Ratner and Allan S. Hoffman. Synthetic hydrogels for biomedical applications. *ACS Symposium Series*, page 1–36, 1976.

[7] Karl G. Wiese. Osmotically induced tissue expansion with hydrogels: a new dimension in tissue expansion? a preliminary report. *Journal of Cranio-Maxillofacial Surgery*, 21(7):309–313, 1993.

[8] Yinping Liu, Lulu Wang, Yuanyuan Mi, Sisi Zhao, Simeng Qi, Meng Sun, Bo Peng, Quan Xu, Yingchun Niu, and Yang Zhou. Transparent stretchable

hydrogel sensors: materials, design and applications. *Journal of Materials Chemistry C*, 10:13351–13371, 2022.

[9] Xuemei Li, Zhiwei Liu, Yongri Liang, Li-Min Wang, and Ying Dan Liu. Chitosan-based double cross-linked ionic hydrogels as a strain and pressure sensor with broad strain-range and high sensitivity. *Journal of Materials Chemistry B*, 10:3434–3443, 2022.

[10] Bowen Yang and Weizhong Yuan. Highly stretchable, adhesive, and mechanical zwitterionic nanocomposite hydrogel biomimetic skin. *ACS Applied Materials & Interfaces*, 11(43):40620–40628, 2019.

[11] Canhui Yang and Zhigang Suo. Hydrogel ionotronics. *Nature Reviews Materials*, 3(6):125–142, 2018.

[12] Chun Zhao, Yanjie Wang, Gangqiang Tang, Jie Ru, Zicai Zhu, Bo Li, Chuan Fei Guo, Lijie Li, and Denglin Zhu. Ionic flexible sensors: Mechanisms, materials, structures, and applications. *Advanced Functional Materials*, 32(17):2110417, 2022.

[13] Michelle L. Oyen. Mechanical characterisation of hydrogel materials. *International Materials Reviews*, 59(1):44–59, 2014.

[14] Michael A. DePierro, Kyle G. Carpenter, and C. Allan Guymon. Influence of polymerization conditions on nanostructure and properties of polyacrylamide hydrogels templated from lyotropic liquid crystals. *Chemistry of Materials*, 18(23):5609–5617, 2006.

[15] Xinyue Liu, Ji Liu, Shaoting Lin, and Xuanhe Zhao. Hydrogel machines. *Materials Today*, 36:102–124, 2020.

[16] Nadia Adrus and Mathias Ulbricht. Rheological studies on PNIPAAm hydrogel synthesis via in situ polymerization and on resulting viscoelastic properties. *Reactive and Functional Polymers*, 73(1):141–148, 2013.

[17] Yuanyuan Bai, Baohong Chen, Feng Xiang, Jinxiong Zhou, Hong Wang, and Zhigang Suo. Transparent hydrogel with enhanced water retention capacity by introducing highly hydratable salt. *Applied Physics Letters*, 105(15):151903, 2014.

[18] Cyrus W. Beh, Dionis S. Yew, Ruth J. Chai, Sau Yin Chin, Yiqi Seow, and Shawn S. Hoon. A fluid-supported 3D hydrogel bioprinting method. *Biomaterials*, 276:121034, 2021.

[19] Lu-Yu Zhou, Jianzhong Fu, and Yong He. A review of 3D printing technologies for soft polymer materials. *Advanced Functional Materials*, 30(28):2000187, 2020.

[20] Yannick Rioux, Julie Fradette, Yvan Maciel, André Bégin-Drolet, and Jean Ruel. Biofabrication of sodium alginate hydrogel scaffolds for heart valve tissue engineering. *International Journal of Molecular Sciences*, 23(15), 2022.

[21] Hui Wang, Biao Zhang, Jianhong Zhang, Xiangnan He, Fukang Liu, Jingjing Cui, Zhe Lu, Guang Hu, Jun Yang, Zhe Zhou, Runze Wang, Xingyu Hou, Luankexin Ma, Panyu Ren, Qi Ge, Peng Li, and Wei Huang. General one-pot method for preparing highly water-soluble and biocompatible photoinitiators for digital light processing-based 3D printing of hydrogels. *ACS Applied Materials & Interfaces*, 13(46):55507–55516, 2021.

[22] Binbin Ying and Xinyu Liu. Skin-like hydrogel devices for wearable sensing, soft robotics and beyond. *iScience*, 24(11):103174, 2021.

[23] Xiaojie Sui, Hongshuang Guo, Chengcheng Cai, Qingsi Li, Chiyu Wen, Xiangyu Zhang, Xiaodong Wang, Jing Yang, and Lei Zhang. Ionic conductive hydrogels with long-lasting antifreezing, water retention and self-regeneration abilities. *Chemical Engineering Journal*, 419:129478, 2021.

[24] Amy E. Emerson, Alec B. McCall, Sarah R. Brady, Emily M. Slaby, and Jessica D. Weaver. Hydrogel injection molding to generate complex cell encapsulation geometries. *ACS Biomaterials Science & Engineering*, 8(9):4002–4013, 2022.

[25] Ying Li, Jeffrey D. Motschman, Sean T. Kelly, and Benjamin B. Yellen. Injection molded microfluidics for establishing high-density single cell arrays in an open hydrogel format. *Analytical Chemistry*, 92(3):2794–2801, 2020.

[26] Haibo Wang, Jun Xiang, Xiao Wen, Xiaosheng Du, Yin Wang, Zongliang Du, Xu Cheng, and Shuang Wang. Multifunctional skin-inspired resilient MXene-embedded nanocomposite hydrogels for wireless wearable electronics. *Composites Part A: Applied Science and Manufacturing*, 155:106835, 2022.

[27] Zhenghao Li, Wenlong Xu, Xinhao Wang, Wenqing Jiang, Xiaolong Ma, Fangjunchuan Wang, Caili Zhang, and Chunguang Ren. Fabrication of PVA/PAAm IPN hydrogel with high adhesion and enhanced mechanical properties for body sensors and antibacterial activity. *European Polymer Journal*, 146:110253, 2021.

[28] M. Toyabur Rahman, S. M. Sohel Rana, M. Salauddin, M. Abu Zahed, Sanghyun Lee, Eui-Sung Yoon, and Jae Yeong Park. Silicone-incorporated nanoporous cobalt oxide and MXene nanocomposite-coated stretchable fabric for wearable triboelectric nanogenerator and self-powered sensing applications. *Nano Energy*, 100:107454, 2022.

[29] Lixin Chen, Jingquan Liu, Xiaolin Wang, Bowen Ji, Xiang Chen, and Bin Yang. Flexible capacitive hydrogel tactile sensor with adjustable measurement range using liquid crystal and carbon nanotubes composites. *IEEE Transactions on Electron Devices*, 64(5):1968–1972, 2017.

[30] Jeong-Yun Sun, Christoph Keplinger, George M. Whitesides, and Zhigang Suo. Ionic skin. *Advanced Materials*, 26(45):7608–7614, 2014.

[31] Max Born. Volumen und hydratationswärme der Ionen. *Zeitschrift für Physik*, 1(1):45–48, 1920.

[32] Marat Andreev, Juan J. de Pablo, Alexandros Chremos, and Jack F. Douglas. Influence of ion solvation on the properties of electrolyte solutions. *The Journal of Physical Chemistry B*, 122(14):4029–4034, 2018.

[33] Yanqing Wang, Picheng Chen, Xinjie Zhou, Yuetao Liu, Ning Wang, and Chuanhui Gao. Highly sensitive zwitterionic hydrogel sensor for motion and pulse detection with water retention, adhesive, antifreezing, and self-healing properties. *ACS Applied Materials & Interfaces*, 14(41):47100–47112, 2022.

[34] Jiajun Xu, Guangyu Wang, Yufan Wu, Xiuyan Ren, and Guanghui Gao. Ultra-stretchable wearable strain and pressure sensors based on adhesive, tough, and self-healing hydrogels for human motion monitoring. *ACS Applied Materials & Interfaces*, 11(28):25613–25623, 2019.

[35] Ren'ai Li, Kaili Zhang, Ling Cai, Guangxue Chen, and Minghui he. Highly stretchable ionic conducting hydrogels for strain/tactile sensors. *Polymer*, 167:154–158, 2019.

[36] Xin Jing, Hao-Yang Mi, Yu-Jyun Lin, Eduardo Enriquez, Xiang-Fang Peng, and Lih-Sheng Turng. Highly stretchable and biocompatible strain sensors based on mussel-inspired super-adhesive self-healing hydrogels for human motion monitoring. *ACS Applied Materials & Interfaces*, 10(24):20897–20909, 2018.

[37] Shuqi Liu, Rongmin Zheng, Song Chen, Yunhui Wu, Haizhou Liu, Pingping Wang, Zhifu Deng, and Lan Liu. A compliant, self-adhesive and self-healing wearable hydrogel as epidermal strain sensor. *Journal of Materials Chemistry C*, 6:4183–4190, 2018.

[38] Jin Wu, Zixuan Wu, Xing Lu, Songjia Han, Bo-Ru Yang, Xuchun Gui, Kai Tao, Jianmin Miao, and Chuan Liu. Ultrastretchable and stable strain sensors based on antifreezing and self-healing ionic organohydrogels for human motion monitoring. *ACS Applied Materials & Interfaces*, 11(9):9405–9414, 2019.

[39] Yue Zhao, Aeree Kim, Guanxiang Wan, and Benjamin C. Tee. Design and applications of stretchable and self-healable conductors for soft electronics. *Nano Convergence*, 6(1), 2019.

[40] Li'an Jiang, Song Tian, Yuhui Xie, Xue Lv, and Shulin Sun. High strength, conductivity, and bacteriostasis of the P(AM-co-AA)/chitosan quaternary ammonium salt composite hydrogel through ionic crosslinking and hydrogen bonding. *Langmuir*, 39(25):8698–8709, 2023.

[41] Haoxiang Zhang, Wenbin Niu, and Shufen Zhang. Extremely stretchable, sticky and conductive double-network ionic hydrogel for ultra-stretchable and compressible supercapacitors. *Chemical Engineering Journal*, 387:124105, 2020.

[42] Lujie Cao, Mingyang Yang, Dong Wu, Fucong Lyu, Zhifang Sun, Xiongwei Zhong, Hui Pan, Hongtao Liu, and Zhouguang Lu. Biopolymer-chitosan based supramolecular hydrogels as solid state electrolytes for electrochemical energy storage. *Chemical Communications*, 53:1615–1618, 2017.

[43] Yunjian Guo, Feifei Yin, Yang Li, Guozhen Shen, and Jong-Chul Lee. Incorporating wireless strategies to wearable devices enabled by a photocurable hydrogel for monitoring pressure information. *Advanced Materials*, 35(29):2300855, 2023.

[44] Jianyu Yin, Shenxin Pan, Lili Wu, Liyina Tan, Di Chen, Shan Huang, Yuhong Zhang, and Peixin He. A self-adhesive wearable strain sensor based on a highly stretchable, tough, self-healing and ultra-sensitive ionic hydrogel. *Journal of Materials Chemistry C*, 8:17349–17364, 2020.

[45] Ruidong Xu, Minghua She, Jiaxu Liu, Shikang Zhao, Jisheng Zhao, Xueji Zhang, Lijun Qu, and Mingwei Tian. Skin-friendly and wearable iontronic touch panel for virtual-real handwriting interaction. *ACS Nano*, 17(9):8293–8302, 2023.

[46] Young Jun Son, Seunghwan Seo, Kyoung-Yong Chun, Jin Woo Bae, Ho Jung Lee, Seonghyun Bae, Seunghyun Baik, and Chang-Soo Han. Stretchable, transparent, and water-resistive touch panel using ion gel. *Sensors and Actuators A: Physical*, 334:113328, 2022.

[47] Hongyan Liu, Xing Wang, Yanxia Cao, Yanyu Yang, Yatian Yang, Yafei Gao, Zhanshan Ma, Jianfeng Wang, Wanjie Wang, and Decheng Wu. Freezing-tolerant, highly sensitive strain and pressure sensors assembled from ionic conductive hydrogels with dynamic cross-links. *ACS Applied Materials & Interfaces*, 12(22):25334–25344, 2020.

[48] Xiaojie Sui, Hongshuang Guo, Chengcheng Cai, Qingsi Li, Chiyu Wen, Xiangyu Zhang, Xiaodong Wang, Jing Yang, and Lei Zhang. Ionic conductive hydrogels with long-lasting antifreezing, water retention and self-regeneration abilities. *Chemical Engineering Journal*, 419:129478, 2021.

[49] Huiyu Bai, Daiwei Chen, Haiyan Zhu, Shengwen Zhang, Wei Wang, Piming Ma, and Weifu Dong. Photo-crosslinking ionic conductive PVA-SbQ/FeCl3 hydrogel sensors. *Colloids and Surfaces A: Physicochemical and Engineering Aspects*, 648:129205, 2022.

[50] Jing Cong, Zhiwei Fan, Shaoshan Pan, Jie Tian, Weizhen Lian, Shan Li, Sijie Wang, Dongchang Zheng, Chunguang Miao, Weiping Ding, Taolin Sun, and Tianzhi Luo. Polyacrylamide/chitosan-based conductive double network hydrogels with outstanding electrical and mechanical performance at low temperatures. *ACS Applied Materials & Interfaces*, 13(29):34942–34953, 2021.

[51] Xinxin Sun, Chunhui Luo, and Faliang Luo. Preparation and properties of self-healable and conductive PVA-agar hydrogel with ultra-high mechanical strength. *European Polymer Journal*, 124:109465, 2020.

[52] Jun Yang, Chun-rui Han, Feng Xu, and Run-cang Sun. Simple approach to reinforce hydrogels with cellulose nanocrystals. *Nanoscale*, 6:5934–5943, 2014.

[53] Fatemeh Ahmadi, Zahra Oveisi, Soliman M. Samani, and Zohreh Amoozgar. Chitosan based hydrogels: characteristics and pharmaceutical applications. *Research in Pharmaceutical Sciences*, 10(1):1–16, 2015.

[54] Shuyu Wang, Zhaojia Sun, Yuliang Zhao, and Lei Zuo. A highly stretchable hydrogel sensor for soft robot multi-modal perception. *Sensors and Actuators A: Physical*, 331:113006, 2021.

[55] Tang Zhu, Chi Jiang, Mingliang Wang, Caizhen Zhu, Ning Zhao, and Jian Xu. Skin-inspired double-hydrophobic-coating encapsulated hydrogels with enhanced water retention capacity. *Advanced Functional Materials*, 31(27):2102433, 2021.

[56] Wenyu Zhao, Zhuofan Lin, Xiaopu Wang, Ziya Wang, and Zhenglong Sun. Mechanically interlocked hydrogel–elastomer strain sensor with robust interface and enhanced water–retention capacity. *Gels*, 8(10):625, 2022.

[57] Biao Zhang, Shiya Li, Hardik Hingorani, Ahmad Serjouei, Liraz Larush, Amol A. Pawar, Wei Huang Goh, Amir Hosein Sakhaei, Michinao Hashimoto, Kavin Kowsari, Shlomo Magdassi, and Qi Ge. Highly stretchable hydrogels for UV

curing based high-resolution multimaterial 3D printing. *Journal of Materials Chemistry B*, 6:3246–3253, 2018.

[58] Qing Gao, Xuefeng Niu, Lei Shao, Luyu Zhou, Zhiwei Lin, Anyu Sun, Jianzhong Fu, Zichen Chen, Jun Hu, Yande Liu, and Yong He. 3D printing of complex GelMA-based scaffolds with nanoclay. *Biofabrication*, 11(3):035006, 2019.

[59] Pramod Dorishetty, Rajkamal Balu, Sandya S. Athukoralalage, Tamar L. Greaves, Jitendra Mata, Liliana de Campo, Nabanita Saha, Andrew C. W. Zannettino, Naba K. Dutta, and Namita Roy Choudhury. Tunable biomimetic hydrogels from silk fibroin and nanocellulose. *ACS Sustainable Chemistry & Engineering*, 8(6):2375–2389, 2020.

[60] Alexandre Xavier Mendes, Saimon Moraes Silva, Cathal D. O'Connell, Serena Duchi, Anita F. Quigley, Robert M. I. Kapsa, and Simon E. Moulton. Enhanced electroactivity, mechanical properties, and printability through the addition of Graphene Oxide to photo-cross-linkable Gelatin Methacryloyl hydrogel. *ACS Biomaterials Science & Engineering*, 7(6):2279–2295, 2021.

[61] Sijun Liu and Lin Li. Ultrastretchable and self-healing double-network hydrogel for 3D printing and strain sensor. *ACS Applied Materials & Interfaces*, 9(31):26429–26437, 2017.

[62] Mohsen Janmaleki, Jun Liu, Milad Kamkar, Milad Azarmanesh, Uttandaraman Sundararaj, and Amir Sanati Nezhad. Role of temperature on bio-printability of gelatin methacryloyl bioink in two-step cross-linking strategy for tissue engineering applications. *Biomedical Materials*, 16(1):015021, 2020.

[63] Xiang-Yu Yin, Yue Zhang, Junfeng Xiao, Carolyn Moorlag, and Jun Yang. Monolithic dual-material 3D printing of ionic skins with long-term performance stability. *Advanced Functional Materials*, 29(39):1904716, 2019.

[64] Yiru Zhang, Lei Chen, Mingzhu Xie, Ziheng Zhan, Dongsheng Yang, Ping Cheng, Huigao Duan, Qi Ge, and Zhaolong Wang. Ultra-fast programmable human-machine interface enabled by 3D printed degradable conductive hydrogel. *Materials Today Physics*, 27:100794, 2022.

[65] Yang Zhou, Yuecheng Cui, and Li-Qun Wang. A dual-sensitive hydrogel based on poly(lactide-co-glycolide)-polyethylene glycol-poly(lactide-co-glycolide) block copolymers for 3D printing. *International Journal of Bioprinting*, 7(3):389, 2021.

[66] Heng Zhu, Xiaocheng Hu, Binhong Liu, Zhe Chen, and Shaoxing Qu. 3D printing of conductive hydrogel–elastomer hybrids for stretchable electronics. *ACS Applied Materials & Interfaces*, 13(49):59243–59251, 2021.

[67] Gangadevi Sennakesavan, Mohammad Mostakhdemin, Lari K. Dkhar, Ali Seyfoddin, and Szali J. Fatihhi. Acrylic acid/acrylamide based hydrogels and its properties - a review. *Polymer Degradation and Stability*, 180:109308, 2020.